

*Birck Nanotechnology Center*  
*Birck and NCN Publications*

---

Purdue Libraries

Year 2008

---

Nanoscale thickness double-gated field  
effect silicon sensors for sensitive pH  
detection in fluid

Oguz H. Elibol\*      Bobby Reddy Jr.†  
Rashid Bashir‡

\*Purdue University - Main Campus, elibol@purdue.edu

†Micro and Nanotechnology Laboratory and Department of Electrical and Computer Engineering, University of Illinois

‡Birck Nanotechnology Center and Bindley Bioscience Center, Purdue University, bashir@purdue.edu

This paper is posted at Purdue e-Pubs.

<http://docs.lib.purdue.edu/nanopub/156>

## Nanoscale thickness double-gated field effect silicon sensors for sensitive pH detection in fluid

Oguz H. Elibol,<sup>1</sup> Bobby Reddy, Jr.,<sup>2</sup> and Rashid Bashir<sup>2,a)</sup>

<sup>1</sup>Birck Nanotechnology Center and School of Electrical and Computer Engineering, Purdue University, West Lafayette, Indiana 47906, USA

<sup>2</sup>Micro and Nanotechnology Laboratory and Department of Electrical and Computer Engineering, University of Illinois at Urbana-Champaign, Urbana, Illinois 61801, USA

(Received 23 March 2008; accepted 16 April 2008; published online 15 May 2008)

In this work, we report on the optimization of a double-gate silicon-on-insulator field effect device operation to maximize pH sensitivity. The operating point can be fine tuned by independently biasing the fluid and the back gate of the device. Choosing the bias points such that device is nearly depleted results in an exponential current response—in our case, 0.70 decade per unit change in pH. This value is comparable to results obtained with devices that have been further scaled in width, reported at the forefront of the field, and close to the ideal value of 1 decade/pH. By using a thin active area, sensitivity is increased due to increased coupling between the two conducting surfaces of the devices. © 2008 American Institute of Physics. [DOI: 10.1063/1.2920776]

Miniaturized sensors play an indispensable role in the downscaling of chemical and biological analysis systems for cost effective and high throughput operation. Besides sensing molecules in fluid, sensing pH in the fluidic environment with high sensitivity is of fundamental importance for chemical and biological applications.<sup>1</sup> Among the types of sensors amenable for miniaturization for such use,<sup>2,3</sup> electrical sensors are very attractive since they can be mass fabricated in a cost effective fashion, individually addressed, integrated with other components on a common platform, and easily interfaced for electrical readout. Electrical sensing can be executed using metal electrodes<sup>4</sup> or by using field effect sensors with a suitable gate dielectric. Field effect sensors offer versatile operation with no electrochemical reactions on the surface, easy surface modification, and a potential to be reused. Using field effect transistors, often referred to as ion-sensitive-field-effect transistors, as charge sensitive elements in fluid, has been pioneered by Bergveld.<sup>5</sup> Recently, there has been a renewed interest and a trend toward further miniaturizing field effect devices, providing better charge sensitivity compared to their bulk counterparts.<sup>6</sup> Here, we report on the operation of a double-gated nanoscale thickness field effect device with microscale width and show that decreasing the thickness of the active area with operating bias optimization yields close to ideal operation for sensing the pH of the fluid environment. We highlight the importance of using both the bottom and fluidic gates and discuss parameters important for the optimization of operation.

A fully complementary metal-oxide semiconductor compatible process was used for the transducer fabrication.<sup>7</sup> As shown in Fig. 1, the typical resulting active area for each “nanoplate” sensor is about 2 μm in width, 20 μm in length, and 27 nm in thickness. The source-drain current ( $I_{DS}$ ) was measured as a function of both the back gate bias ( $V_{BS}$ ) and fluid gate bias ( $V_{FS}$ ) for buffers with different pH values.<sup>7</sup> The substrate bias is used as a back gate, and the fluid bias is controlled by biasing the platinum contacting the fluid at the front surface (Fig. 1). Figure 2(a) qualitatively describes the

mode of operation under various biasing conditions. Using a silicon-on-insulator (SOI) device instead of a bulk device allows for operation in both inversion and accumulation modes, by applying a positive bias or negative bias, respectively, to the fluid and back gate. In full inversion or depletion, fixing the bias at one of the gates and shifting the other gate potential toward flatband (toward the center), causes the device to become partially depleted. For sensing purposes, this mode, known as the subthreshold region, is the choice of

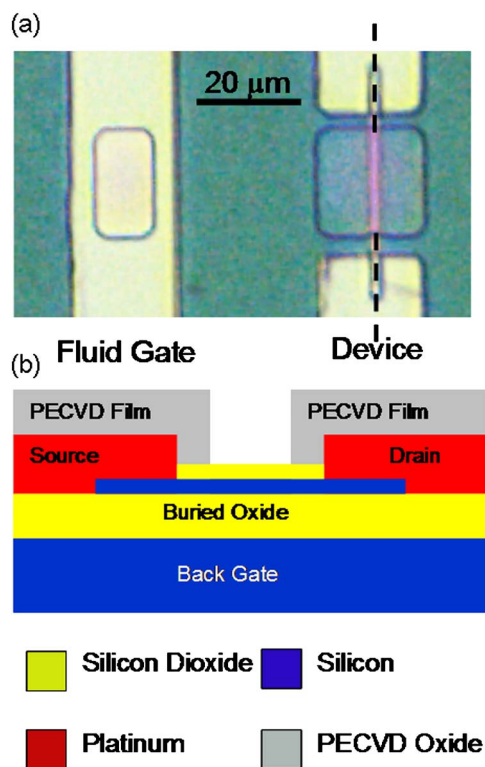


FIG. 1. (Color online) (a) Optical micrograph shows the platinum fluidic gate near a device on the chip. Both a fluidic gate and a back gate are used to modulate the conduction properties of the device, resulting in a double-gated field effect sensor. (b) Schematic representation of the cross section of a nanoplate device through the dashed lines shown in (a), illustrating the final material composition and geometry of the sensor.

<sup>a)</sup>Electronic mail: rbashir@uiuc.edu.

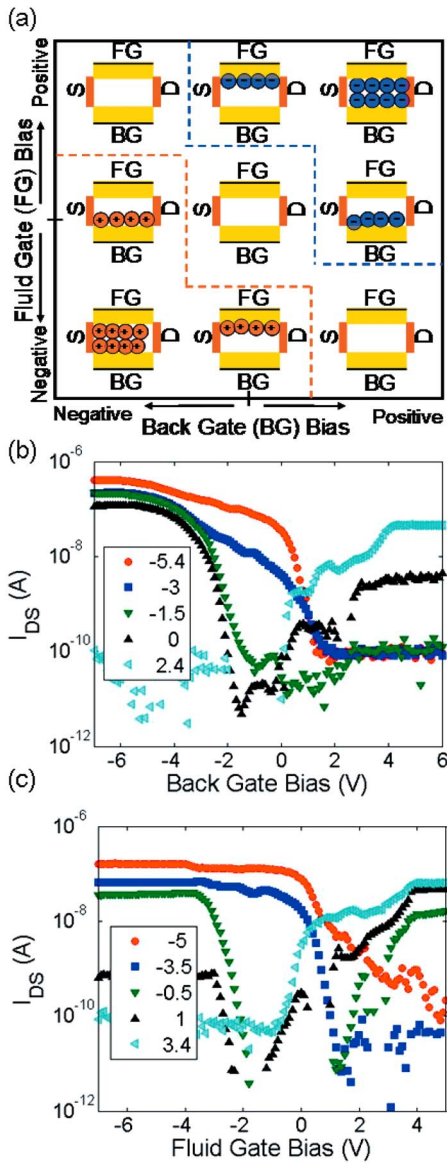


FIG. 2. (Color online) (a) Qualitative description of the device operation modes as a function of the fluid and back gate bias of the device (potentials with respect to source potential). Red circles represent holes and blue circles represent electrons. Depending on the bias applied, the device can be fully depleted (opposing polarities of fluid and gate bias, or no bias), fully accumulated (negative fluid and back gate bias), fully inverted (positive fluid and back gate bias) or partially depleted (biasing one gate, and not biasing the other). (b)  $I_{DS}$  as a function of the back gate bias ( $V_{BS}$ ) at different fluid gate gate biases ( $V_{FS}$ -shown in the legend in volts). (c)  $I_{DS}$  as a function of the fluid gate bias ( $V_{FS}$ ) at different back gate gate biases ( $V_{BS}$ -shown in the legend in volts).

operation since the change in current is exponential for a linear change in surface potential. The red and blue dashed lines in Fig. 2(a) highlight these regions that are optimum for operation as a sensor. The source-drain current through the device for different gate biases corresponding to each of the different modes in Fig. 2(a) is shown in Figs. 2(b) and 2(c).

In order to identify the optimum operating conditions of the sensor,  $I_{DS}$  was measured as a function of both the fluid and back gate voltages, in 10 mM sodium phosphate buffer with pH 8.10. A slight expected drift in the current due to the formation of the double layer and the hydration of the silicon dioxide layer was observed<sup>8</sup> and measurements were taken until drift was minimized [Fig. 3(a)]. The fluid was replaced with the same buffer at pH 6.31, and current was measured

once again<sup>7</sup> [Fig. 3(b)]. Bias conditions for maximum sensitivity were identified by dividing  $I_{DS}$  at pH 8.10 by  $I_{DS}$  at pH 6.31 and plotting the logarithm of the result as a function of the fluid and back gate bias [Fig. 3(c)-equivalent of subtracting Fig. 3(a) from Fig. 3(b)]. Maximum sensitivity is observed at the hole and electron conduction shores, as was previously explained [Fig. 2(a)]. Taking the weighted sum of two parts, (1) partial derivative of  $I_{DS}$  with respect to  $V_{FS}$  and (2) partial derivative of  $I_{DS}$  with respect to  $V_{BS}$  at pH 8.10, reasonably predicts the most sensitive regions [Fig. 3(d)].

The fluid potential ( $V_{FS}$ ) directly modulates the top surface potential ( $Y_F$ ). Hence, taking  $(d \log_{10}(I_{DS})/dV_{FS})$  will correctly predict the sensitivity to surface charge. However this is not possible with a dc measurement system since only partial derivatives with respect to one variable can be obtained, not the direct derivative. In order to obtain the direct derivative from dc measurements the magnitude of coupling (c) of the two surfaces should be known,

$$\frac{d \log(I_{DS})}{dV_{FS}} = \frac{\partial \log(I_{DS})}{\partial V_{FS}} + \frac{\partial \log(I_{DS})}{\partial V_{BS}} \cdot \frac{dV_{BS}}{dV_{FS}}, \quad (1)$$

where the coupling coefficient is

$$\frac{dV_{BS}}{dV_{FS}} = c. \quad (2)$$

The relative contribution of the two partial derivatives in (1) to the final sensitivity can be taken as a measure of how much the two surfaces are coupled ( $c$ ) to each other. In the case in which the conduction channel is much thicker than the intrinsic Debye length ( $t_{\text{channel}} \gg L_D$ ), the front and back surfaces will be totally decoupled from each other, and the sensitivity to change in charge on the front surface (electrolyte-insulator interface) will only be represented by the first part (partial with respect to  $V_{FS}$ ). Alternatively, in the case in which the thickness is small compared to the intrinsic Debye length ( $t_{\text{channel}} \ll L_D$ ), the contribution of the two parts will be the same (partial with respect to  $V_{FS}$  and  $V_{BS}$ ). In our case, the intrinsic Debye length is about the same as the thickness of the active area (both about 30 nm,  $t_{\text{channel}} \sim L_D$ ). Hence, the first part is expected to have a greater contribution than the second part. The effect of this nonequal contribution can be seen by comparing Figs. 3(c) and 3(d), as the contribution from the second part overestimates the sensitivity in certain regions [shown with a black dashed ellipse in Fig. 3(d)]. The coupling of the front to back surfaces changes as a function of the gate biases (changing the carrier concentration), also affecting the sensitivity of the device.<sup>7</sup> The method presented for estimating the optimum biasing conditions can be used for any SOI or nanowire device in which the back gate and fluid bias can be controlled.

The source-drain current measured at different biasing conditions highlights the effect of operation conditions on the sensitivity. For example, biasing the device at one point yields a sensitivity of 0.50 decade/pH [Fig. 3(e)], while another bias condition yields a sensitivity of 0.70 decade/pH [Fig. 3(f)]. It is evident that transducer performance increases as the device is biased closer to depletion in the subthreshold region of the device.

The subthreshold slope for a field effect device is given by the equation<sup>9</sup>

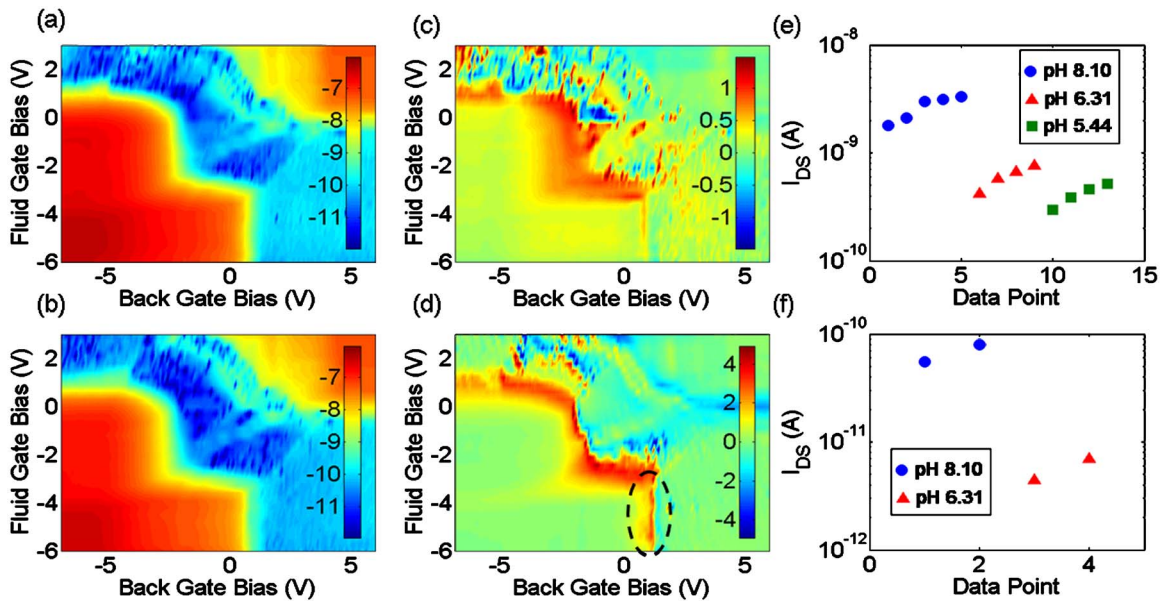


FIG. 3. (Color online) (a)  $\log_{10}(I_{DS})$  (magnitude shown with the color bar) as a function of the fluid and back gate biases with device operating in 10 mM sodium phosphate buffer at pH 8.10. (b) same as (a) in pH 6.31 (c) Logarithmic ratio of  $I_{DS}$  at pH 8.10 to  $I_{DS}$  at pH 6.31 (magnitude shown with the color bar) as the experimental verification of the surface charge sensitivity of the device. (d) Sum of partial derivative of  $I_{DS}$  with respect to  $V_{FS}$  and (0.5) times the partial derivative of  $I_{DS}$  with respect to  $V_{BS}$  at pH 8.10 (magnitude shown with the color bar) as a measure of device sensitivity to change in surface charge. (e)  $I_{DS}$  as a function of the buffer pH, at  $V_{BS}=-2.4$  V and  $V_{FS}=-0.3$  V. Data points are consecutive in time, separated by approximately 15 min. (f) Same as (e), but operating at  $V_{BS}=-0.8$  V and  $V_{FS}=-2.4$  V.

$$S = [d(\log_{10}(I_{DS}))/dV_{GS}]^{-1} = 2.3mkT/q, \quad (3)$$

where  $k$  is the Boltzmann constant,  $T$  is the temperature,  $q$  is the charge of a single electron, and  $m$  is a factor (with a minimum value of 1) which describes the degree of control of the gate over the channel region. The value of an ideal  $S$  at room temperature is approximately  $m$  times 60 mV/decade. It is also well established that the surface potential change of  $\text{SiO}_2$  as a function of pH ranges from 40–60 mV/pH depending on the density and activation of surface sites, buffer ionic strength, and composition.<sup>10</sup> In the ideal case, a purely Nernstian response will give a surface potential sensitivity of  $2.3kT/q$  V/pH,<sup>11</sup> which places a fundamental limit on the best case sensitivity. Change in current is limited to at most one decade per one unit pH change of the buffer (1 decade/pH). This work has demonstrated that it is possible to obtain 0.70 decade/pH using nanoplate sensors, which is similar to the sensitivities reported with other work at the forefront of the field. Nanoscale width silicon transducers such as nanowires are reported to have sensitivities such as 0.82,<sup>12</sup> 0.06,<sup>13</sup> and 0.007 decade/pH.<sup>14</sup> Work with other SOI structures report 0.19 decade/pH (Ref. 15) and 0.04 decade/pH.<sup>16,7</sup> It should also be noted that the sensitivity can be improved by optimizing the fabrication and reducing the interface trap densities of the devices.

This leads us to conclude that the sensitivity to pH that can be obtained with microscale widths and nanoscale thickness field effect transducers can be close to the fundamental limit, especially when used in a double gate mode with optimization of biasing conditions. Our experiments demonstrated the importance and benefits of using a double-gated device to choose the optimum fluid and substrate bias conditions for maximum sensitivity. For an active area thin enough compared to the intrinsic Debye length, using the

combination of the partial derivatives of the source-drain current with respect to the back and fluid bias was found to be a good estimator for determining the optimum biasing conditions.

- <sup>1</sup>R. Bashir, J. Z. Hilt, O. Elibol, A. Gupta, and N. A. Peppas, *Appl. Phys. Lett.* **81**, 3091 (2002).
- <sup>2</sup>D. G. Hafeman, J. W. Pierce, and H. M. McConnell, *Science* **240**, 1182 (1988).
- <sup>3</sup>S. R. Manalis, E. B. Cooper, P. F. Indermuhle, P. Kernan, P. Wagner, D. G. Hafeman, S. C. Minne, and C. F. Quate, *Appl. Phys. Lett.* **76**, 1072 (2000).
- <sup>4</sup>S. Glab, A. Hulanicki, G. Edwall, and F. Ingman, *Crit. Rev. Anal. Chem.* **21**, 29 (1989).
- <sup>5</sup>P. Bergveld, *IEEE Trans. Biomed. Eng.* **BME-19**, 342 (1972).
- <sup>6</sup>N. Elfstrom, R. Juhasz, I. Sychugov, T. Engfeldt, A. E. Karlstrom, and J. Linnros, *Nano Lett.* **9**, 2608 (2007).
- <sup>7</sup>See EPAPS Document No. E-APPLAB-92-010319 for experimental protocol. For more information on EPAPS, see <http://www.aip.org/pubservs/epaps.html>.
- <sup>8</sup>C. D. Fung, P. W. Cheung, and W. H. Ko, *IEEE Trans. Electron Devices* **33**, 8 (1986).
- <sup>9</sup>Y. Taur and T. H. Ning, *Fundamentals of Modern VLSI Devices* (Cambridge University Press, Cambridge, 1998), p. 128.
- <sup>10</sup>T. Mikolajick, R. Kuhnhold, R. Schnupp, and H. Ryssel, *Sens. Actuators B* **58**, 450 (1999).
- <sup>11</sup>L. Bousse, N. F. De Rooij, and P. Bergveld, *IEEE Trans. Electron Devices* **10**, 1263 (1983).
- <sup>12</sup>E. Stern, J. F. Klemic, D. A. Routenberg, P. N. Wyrembak, D. B. Turner-Evans, A. D. Hamilton, D. A. LaVan, T. M. Fahmy, and M. A. Reed, *Nature (London)* **445**, 519 (2007).
- <sup>13</sup>Y. Cui, Q. Wei, H. Park, and C. M. Lieber, *Science* **293**, 1289 (2001).
- <sup>14</sup>Y. Chen, X. Wang, S. Erramilli, P. Mohanty, and A. Kalinowski, *Appl. Phys. Lett.* **89**, 223512 (2006).
- <sup>15</sup>B. Ashcroft, B. Takulapalli, J. Yang, G. M. Laws, H. Q. Zhang, N. J. Tao, S. Lindsay, D. Gust, and T. J. Thornton, *Phys. Status Solidi B* **241**, 2291 (2004).
- <sup>16</sup>M. G. Nikolaidis, S. Rauschenbach, and A. R. Bausch, *J. Appl. Phys.* **95**, 3811 (2004).